

Bendable ITO-free Organic Solar Cells with Highly Conductive and Flexible PEDOT:PSS Electrodes on Plastic Substrates

Xi Fan,[†] Jinzhao Wang,[‡] Hanbin Wang,[†] Xiang Liu,[†] and Hao Wang^{*,†}

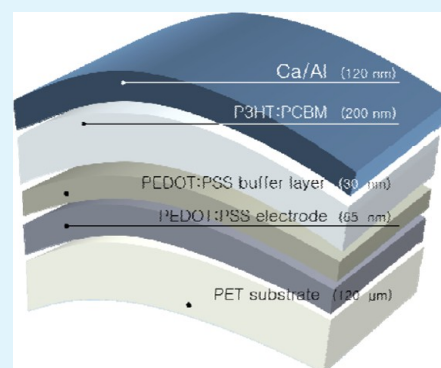
[†]Hubei Collaborative Innovation Center for Advanced Organic Chemical Materials, Faculty of Physics and Electronic Science, Hubei University, Wuhan 430062, People's Republic of China

[‡]Department of Material Science and Engineering, Hubei University, Wuhan 430062, People's Republic of China

S Supporting Information

ABSTRACT: Flexible and transparent electrodes have great potential for photon transmission and charge-carrier collection for next generation electronics compared to rigid electronics with indium tin oxide (ITO)-coated glass substrates. This study describes a comprehensive study of the electrical, morphological, optical, structural, and mechanical properties of poly(3,4-ethylenedioxythiophene):poly(styrenesulfonate) (PEDOT:PSS) films treated by methanol and methanesulfonic acid (MSA), which are coated on hydrophobic flexible plastic substrates. Such a film coated on hydrophobic plastic substrates exhibits a high conductivity up to 3560 S cm⁻¹ and a good mechanical flexibility. Moreover, the use of the films to fabricate bendable ITO-free organic solar cells (OSCs) integrated on plastic substrates was presented. The bendable devices based on P3HT:PCBM not only exhibit a high power conversion efficiency (PCE) up to 3.92%, which is comparable to 4.30% of the rigid devices with ITO-coated glass substrates, but also keep about 80% in PCE of the initial value after 100 time bending with a bending radius of 14 mm in the ambient atmosphere. This work provides a novel route to dramatically improve the conductivity of PEDOT:PSS electrodes, as well as the mechanical flexibility of highly efficient organic electronics with the flexible electrodes.

KEYWORDS: flexible electrodes, PEDOT:PSS, conductivity, plastic substrates, organic solar cells



1. INTRODUCTION

Flexible, transparent and conductive electrodes (TCEs) are one of the most key components for next generation bendable electronics. Indium tin oxide (ITO) is commonly used as a rigid TCE in the electronics, such as organic solar cells (OSCs), organic light-emitting diodes, electronic paper, touch panel displays, and so on, mainly due to its low sheet resistance (R_{sq}) on glass substrates (below 20 Ω sq⁻¹) and high transparency at viable wavelength ranges of 400–800 nm. However, the ITO technology has several drawbacks, including high cost of sputtering deposition in high-temperature processing, low conductivity (σ) on plastic substrates, and a tendency to crack sharply when bent, which seriously hinders its practical application in bendable organic electronics.^{1–3} Therefore, alternative materials with a high conductivity and a good mechanical flexibility become an urgent need in the next-generation bendable electronics.

Several emerging materials have shown promise for the replacement of ITO films and have the potential for large-area coverage and some degree of mechanical compliance. These materials include conducting polymers,^{4–16} carbon nanotubes,^{17–19} graphene,^{20–22} and metallic nanowires.^{23–25} Recently, a cheap, solution-processed, transparent, and conducting polymer, poly(3,4-ethylenedioxythiophene):poly(4-styrenesulfonate) (PEDOT:PSS), was under intense investigation.^{4–16} As-cast PEDOT:PSS films have high transparency

in visible ranges, stable tensile strain, and excellent thermal stability. However, PSS is an insulator that causes a low conductivity of the pristine PEDOT:PSS films. Besides, the crystallinity of PEDOT is not high enough for the strong capacities of charge-carrier transport and collection by electrodes. Thus, the PEDOT:PSS films commonly have a conductivity below 1.0 S cm⁻¹, which is much lower than that of ITO. To achieve a highly conductive film, one method was adding organic compounds, such as ethylene glycol (EG), sorbitol, dimethyl sulfoxide, dimethylformamide, methanol, ethanol, fluorosurfactant, and so on, into PEDOT:PSS aqueous solution,^{6,26–31} whereas an alternate method was dropping polar organic compounds, salt, acid, zwitterions, and solvents, onto the pristine PEDOT:PSS films.^{4,6,7,32–34} Among these methods, sulfuric acid (H₂SO₄) treatments have been considered as very promising methods for the films with a high conductivity and transparency, since a series of conductivity records (3065 S cm⁻¹ and 4380 S cm⁻¹) were reported recently via dropping H₂SO₄ aqueous solutions or 100% H₂SO₄ onto the pristine PEDOT:PSS films and then thermal annealing.^{4,34} However, all the PEDOT:PSS films were prepared on glass substrates and were thermal-annealed at a

Received: April 3, 2015

Accepted: July 10, 2015

Published: July 10, 2015

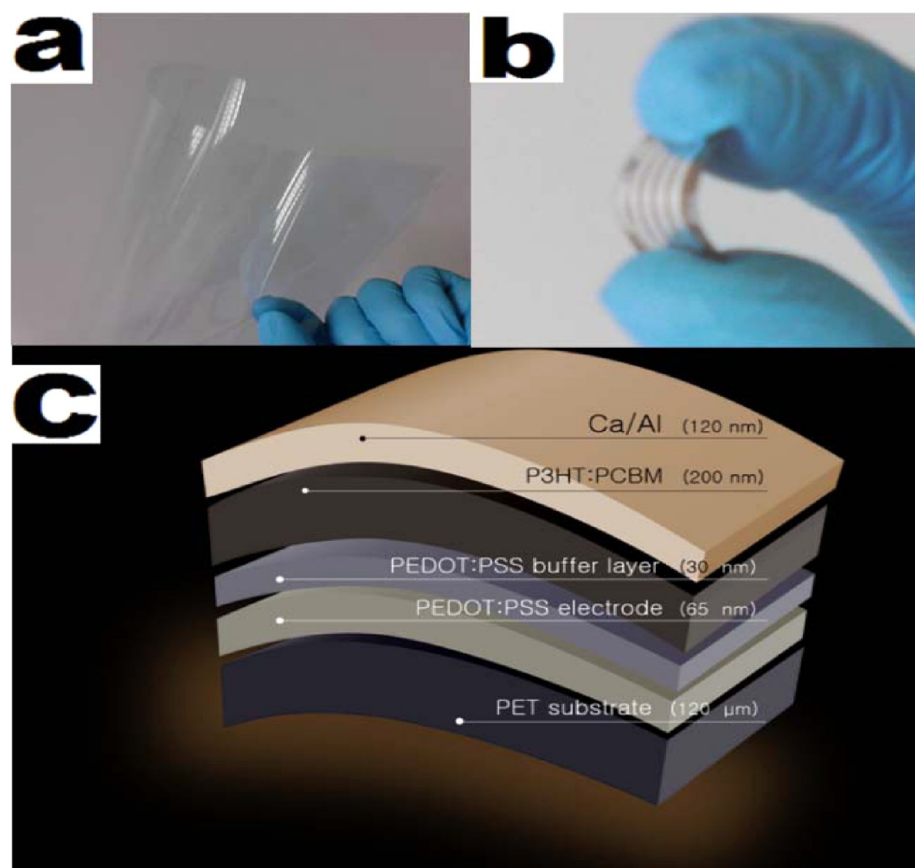


Figure 1. (a) Picture of the PET plastic substrates. (b) Picture of the bendable OSC on the PET substrates. (c) Schematic diagram of the bendable OSC structure.

high temperature of 140–160 °C to obtain high-quality films with a low resistance and a high transmittance. Thus, it is still challenging to prepare the high-quality films on plastic substrates (e.g., polyethylene terephthalate (PET) substrates) due to H_2SO_4 is a very strong, corrosive, and strong oxidizing acid, which can react with plastic substrates, especially under high temperatures, thus causing a large loss in flexibility and transparency of the films. Moreover, H_2SO_4 also cause serious environment pollution problem and risks to human beings.³⁵ In addition, unlike glass substrates, plastic substrates commonly have a hydrophobic nature. It can induce less crystalline PEDOT and more defects in the films after directly dipping and spinning PEDOT:PSS aqueous solutions on plastic substrates; therefore, the conductivity of the PEDOT:PSS films was significantly reduced.

In this study, first, Zonyl FS-300 fluorosurfactant was added into the PEDOT:PSS solutions to enhance the wetting property of the PEDOT:PSS droplets as well as the flexibility of the pristine PEDOT:PSS films. Then, a milk acid solution, 8 M methanesulfonic acid (MSA) aqueous solution was used instead of H_2SO_4 . However, the optimized PEDOT:PSS films on the PET substrates just exhibit a conductivity of 2480 S cm^{-1} , although an increase in conductivity was observed and no remarkable reaction occurred between MSA and PET substrates, even under a high temperature up to 130 °C. Bendable electronics with the PEDOT:PSS films still suffer from the modest conductivity of the films. Here, a pretreatment of 6 vol % methanol and a post-treatment of 8 M MSA were carried out together to improve the conductivity of the PEDOT:PSS films. The combined treatment of methanol/

MSA is an effective and promising method for the conductivity improvement of the films. It produced a highly conductive TCE with a conductivity of 4800 S cm^{-1} ($R_{\text{sq}} \approx 32 \Omega \text{ sq}^{-1}$) on glass substrates. 4800 S cm^{-1} is the highest value of the PEDOT:PSS films, so far, in literature. Even the films were prepared on PET plastic substrates, the conductivity still reaches to 3560 S cm^{-1} . Furthermore, 6 vol % EG was used instead of the 6 vol % methanol. The PEDOT:PSS films with the combined treatment of EG/MSA also exhibit a high conductivity, demonstrating the universality and advance of the method.

Otherwise, although the PEDOT:PSS films reportedly have good electrical, optical, and flexible properties, a detailed investigation of the mechanical flexibility of the PEDOT:PSS films by acid treatments and alcohol/acid combined treatments, and corresponding electronics is still lacking at present. In this study, an exact study of the mechanical flexibility of PEDOT:PSS films treated by methanol and MSA is investigated carefully. Our results demonstrate that the PEDOT:PSS films can be employed for efficient and bendable ITO-free organic solar cells, especially since the remarkable improvement in conductivity has been observed on the flexible plastic substrates.

2. EXPERIMENTAL SECTION

2.1. Preparation and Characterization of PEDOT:PSS Films.

ITO glasses with a sheet resistance of 10 $\Omega \text{ sq}^{-1}$ and 120 μm thick PET plastic substrates (see Figure 1a) were purchased from CSG HOLDING Co., Ltd. (China), and from DuPont Teijin, respectively. The ITO glass was cleaned by sequential ultrasonic treatment in detergent, deionized (DI) water, acetone, and isopropyl alcohol, and

then treated in an ultraviolet-ozone chamber for 15 min. The PET substrates with an area of $1.5 \times 1.5 \text{ cm}^2$ were cleaned by sequential ultrasonic treatment in detergent, DI water, and isopropyl alcohol. The PEDOT:PSS aqueous solutions (Clevios PH1000, mixed with 6 vol % methanol and 6 vol % EG, respectively, and mixed with 0.5 vol % Zonyl FS-300 fluorosurfactant from Fluka) were spin-coated at 2500 rpm for 60 s on the PET substrates to form the PEDOT:PSS films. Then, the films were immersed in methanol and EG for a while, respectively, and then were thermal-annealed on a hot plate in the ambient atmosphere at 120 °C for 10 min. Afterward, the MSA treatment was performed by dropping 8 M MSA aqueous solution on the PEDOT:PSS films on a hot plate at 130 °C for 5 min. Finally, the films were washed by DI water three times, and then were thermal-annealed at 120 °C for 10 min.

Film thickness was measured by a surface profile-meter (Talysurf Series II). Electrical contacts were made by pressing indium on the four corners of each PEDOT:PSS film. Conductivity of all the films was measured by the van der Pauw four-point probe technique with a Keithley 2400 source/meter. Atomic force microscopy (AFM) images of the films were obtained using a Veeco NanoScope IV Multi-Mode AFM with the tapping mode. Transmission spectra were taken on a Hitachi U-3010 UV-visible spectrophotometer. X-ray diffraction (XRD) patterns of the four-layer PEDOT:PSS films were measured with a Bruker D8 Advance with $\text{Cu K}\alpha$ ($\lambda = 1.5406 \text{ \AA}$) at 40 kV and 50 mA.

2.2. Fabrication and Characterization of OSC devices. The bendable OSCs (Figure 1b) and the rigid OSCs were fabricated using the highly conductive PEDOT:PSS films and the 110 nm thick ITO films as an anode, which is coated on PET substrates and on glasses, respectively. Then, PEDOT:PSS (Clevios P VP 4083) solutions were spin-coated at 5000 rpm for 60 s on the electrodes as a buffer layer prior to the active layer deposition. The blend solution of P3HT and PCBM in *ortho*-dichlorobenzene (DCB; 1:1 w/w, 34 mg mL^{-1} for P3HT:PCBM) was spin-coated on top of the PEDOT:PSS buffer layer at 600 rpm for 60 s in a nitrogen filled glovebox. The wet P3HT:PCBM blend films were then placed into glass Petri dishes to undergo solvent annealing. Subsequently, the negative electrode consisting of Ca ($\sim 20 \text{ nm}$) capped with Al ($\sim 100 \text{ nm}$) was thermally evaporated onto the active layer under a shadow mask at a base pressure of about 10^{-4} Pa . The active area is 11 mm^2 for all the OSC devices discussed in this work. Figure 1c show the schematic diagram of the bendable OSC structure. The current-density–voltage (J – V) measurement of the devices was conducted on a computer-controlled Keithley 236 Source Measure Unit. Device characterization was carried out in an ambient atmosphere under illumination of AM1.5G, 100 mW cm^{-2} using a xenon-lamp-based solar simulator (Newport Co., Ltd.). The external quantum efficiency (EQE) was measured with a Stanford Research Systems model SR830 DSP lock-in amplifier coupled with a WDG3 monochromatic outfit and a 500 W xenon lamp. The light intensity at each wavelength was calibrated with a standard single-crystal Si photovoltaic cell.

3. RESULTS AND DISCUSSION

3.1. Effect of Alcohols and MSA on Conductivity of PEDOT:PSS Films. It has been reported that via immersing pristine PEDOT:PSS films in alcohols or dropping small amounts of alcohols into PEDOT:PSS solutions, the electronic conductivity of the films were enhanced. Whereas the pristine PEDOT:PSS films were treated with highly concentrated acids, H^+ easily ionized from the acids and combined the PSS^- of the films to form neutral PSSH. The Columbic attraction disappeared when the PSS chains became PSSH chains by taking protons from the acids and other PSS chains. These PSSH chains could segregate from the film matrix and were removed by washing with DI water. The PSSH chains are neutral and have not any Columbic interaction with PEDOT, so phase separation occurs between the hydrophilic PSSH and hydrophobic PEDOT chains.^{4,34,35} Because the phase separa-

tion of PEDOT:PSS films and the crystallinity of PEDOT were determined by the treatment of $-\text{OH}$ groups of alcohols and the treatment of acids, the conductivity of the films is expected to enhance further after the combined treatment of alcohols and acids.

The conductivity of PEDOT:PSS films is generally evaluated by the van der Pauw four-point probe technique. To calculate the conductivity of the films treated by the alcohols and the MSA, the resistance (R) of the films was measured. The graphs regarding testing the R values of the films on glass substrates are given in Figure S1 (Supporting Information), and t is the thickness of each PEDOT:PSS film.

R_{sq} and σ were calculated by using the following formulas:

$$R_{\text{sq}} = \frac{\pi}{\ln 2} R \quad (1)$$

$$\sigma = \frac{1}{R_{\text{sq}} t} \quad (2)$$

It presents that the thickness of the alcohol-treated PEDOT:PSS films has a slight decrease upon the subsequent post-treatment of the MSA. Table 1 summarizes the results of

Table 1. Sheet Resistance, Conductivity, and Thickness of the PEDOT:PSS Films on Glass and PET Substrates

	EG	methanol	MSA	EG/ MSA	methanol/ MSA
R_{sq} ($\Omega \text{ sq}^{-1}$) ^a	79	65	46	33	32
R_{sq} ($\Omega \text{ sq}^{-1}$) ^b	120	83	62	45	43
σ (S cm^{-1}) ^a	1680	2050	3340	4660	4800
σ (S cm^{-1}) ^b	1110	1600	2480	3420	3560
t (nm)	75 ± 4	75 ± 4	65 ± 3	65 ± 3	65 ± 3

^aOn glass substrates. ^bOn PET substrates.

sheet resistance, conductivity and thickness of the films, which were coated on glass substrates and on PET substrates, respectively. It shows a conductivity of 1680 S cm^{-1} with a sheet resistance of $79 \text{ } \Omega \text{ sq}^{-1}$ for the EG-treated films, 2050 S cm^{-1} with a sheet resistance of $65 \text{ } \Omega \text{ sq}^{-1}$ for the methanol-treated films, and 3340 S cm^{-1} with $46 \text{ } \Omega \text{ sq}^{-1}$ for the MSA-treated films, respectively. With the combined treatments, the conductivity increases significantly to 4660 S cm^{-1} for the EG/MSA treated films and to 4800 S cm^{-1} for the methanol/MSA treated films. The conductivity of 4800 S cm^{-1} is the highest value for the PEDOT:PSS films on glass substrates reported in literature so far. The results display that both the treatments of EG/MSA and methanol/MSA clearly increase drastically the conductivity of the PEDOT:PSS films, which behave almost like a metal. In addition, the conductivity of the films on PET plastic substrates was investigated. It displays that the films on the PET substrates exhibit a lower conductivity, as compared to the PEDOT:PSS films on ultraviolet–ozone-treated glass substrates, probably due to a relatively poor binding property of the PEDOT:PSS droplets to the surface of the plastic substrates. However, the methanol/MSA-treated films on PET still exhibit a conductivity of 3560 S cm^{-1} with a sheet resistance of $43 \text{ } \Omega \text{ sq}^{-1}$. The sheet resistance is lower than the typical sheet resistance of $50 \text{ } \Omega \text{ sq}^{-1}$ of the ITO anodes coated on PET substrates.

3.2. Effect of Alcohols and MSA on Morphology of PEDOT:PSS Films. After the alcohol treatments and the H_2SO_4 treatments in previous literature, the PEDOT:PSS films

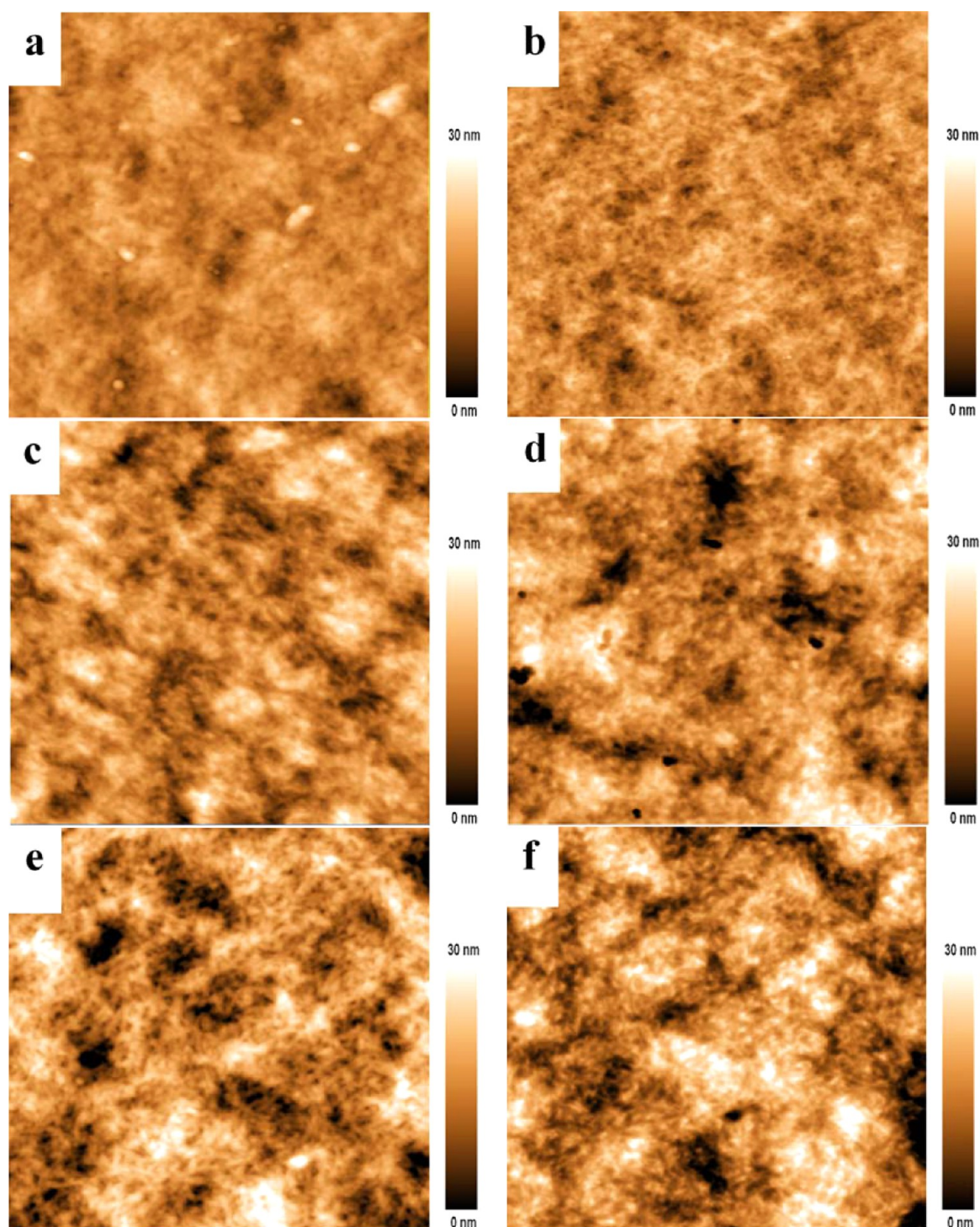


Figure 2. AFM images of the PEDOT:PSS films on PET plastic substrates: (a) pristine films; (b) methanol-treated films; (c) EG-treated films; (d) MSA-treated films; (e) methanol/MSA-treated films; (f) EG/MSA-treated films.

had many fibrils and grains for charge carrier collection by electrodes, which reduced energy barriers and made the free charge-carrier hopping. Thus, the morphology of the PEDOT:PSS films plays a critical role on the enhancement in conductivity of the films. It is worth noting that the PEDOT:PSS aqueous solutions (Clevios PH1000) were filtered through $0.45\ \mu\text{m}$ syringe filter before spin coating. In this work, to avoid some loss of the conductive PEDOT in as-cast films, we did not filter any PEDOT:PSS aqueous solution.

Figure 2 shows the atomic force microscopy (AFM) images of the PEDOT:PSS films. The as-cast PEDOT:PSS films without filtering presents a poor surface with a root-mean-square (RMS) of 5.809 nm, and PEDOT networks were not observed in Figure 2a. However, after the alcohol treatments, it exhibits a smoother surface with a RMS of 3.403 nm for the 6 vol % methanol-treated films and 4.515 nm for the 6 vol % EG-treated films (Figure 2b,c). Moreover, the methanol-treated and EG-treated films present a well-distributed PEDOT networks and small particle aggregates. Figure 2d shows the morphology

of the MSA treated PEDOT:PSS films with a RMS of 6.662 nm. Many black domains are shown in the films, suggesting a disconnected PEDOT in some regions and more removal of PSS from the films, as compared to the alcohols-treated PEDOT:PSS films, whereas there was a better phase separation between PEDOT and PSS and more interconnected conductive PEDOT chains in the methanol/MSA treated films with a RMS of 6.268 nm and the EG/MSA-treated films with a RMS of 6.365 nm, as shown in Figure 2e,f, indicating the further removal of PSS from the films by the subsequent post-treatment of MSA. These findings suggest a generation of high-oriented PEDOT and a depletion of insulating PSS in the PEDOT-rich films with the combined treatments, which result in the improvement in conductivity of the films. Additionally, after the subsequent post-treatment of MSA, the rough films may serve as a center for the initial crystallization of PEDOT, leading to better alignment of PEDOT domains,^{6,36} which was evidenced by the XRD measurement below.

3.3. Effect of Methanol and MSA on Transparency and Crystallinity of PEDOT:PSS Films. The transparency of the PEDOT:PSS films, which is mostly determined by the thickness of the films, is sensitively dependent on its spin-coating speeds. In this work, the spin-coating speed of the PEDOT:PSS (Clevios PH 1000) solutions is 2500 rpm for a better device performance. Noteworthy, the transparency of the PEDOT:PSS films on glass substrates and on PET substrates are almost identical, revealing that the substrates hardly affects the transparency of the PEDOT:PSS films. To understand the effect of the methanol and MSA treatments on the optical and structural properties of the PEDOT:PSS films, we present the transparent spectra and the XRD spectra of the films. All the films were spin-cast with the same spin-coating speed to ensure the initial thicknesses to be constant.

Figure 3a shows the transparent spectra of the glass substrates and the PET substrates in the visible range of 400–800 nm. It displays that the transparency of the PET substrates is superior to that of the ITO-free glass in the visible range of 405–800 nm, especially the PET substrate presents a high transmittance of 97% at 800 nm, which is higher than the transmittance (92%) of the glass substrate. The transparent PET substrates benefits for the fabrication of efficient tandem OSCs that can absorb more visible–NIR lights, due to more photon utilized by photoactive layers. Figure 3b shows the transparent spectra of the PEDOT:PSS films on the PET substrates in the visible range. The transmittance of the 75 nm thick PEDOT:PSS films treated by methanol is 82.5% at 600 nm. It decreases from 91.5 to 70.5% with the increase of the wavelength from 400 to 800 nm. The transmittance of the 65 nm thick PEDOT:PSS film treated by MSA is more than 87.5% in the wavelength below 600 nm, suggesting a relatively high transparency of the films by the MSA treatment, whereas the 65 nm thick PEDOT:PSS films treated by methanol/MSA show a transmittance of 89.5% at the wavelength of 600 nm. Thus, both the MSA-treated films and the methanol/MSA-treated films show a higher transparency than the methanol-treated films. The high transparency may be ascribed to the more removal of PSS from the film matrix, which is beneficial to the achievement of highly conductive PEDOT:PSS films. Besides, the thickness of the ITO films on the glass is about 110 nm, while the thicknesses of the treated PEDOT:PSS films are not more than 75 nm. Thus, the optical transparent coefficient of the PEDOT:PSS films used here is lower than that of the ITO films.

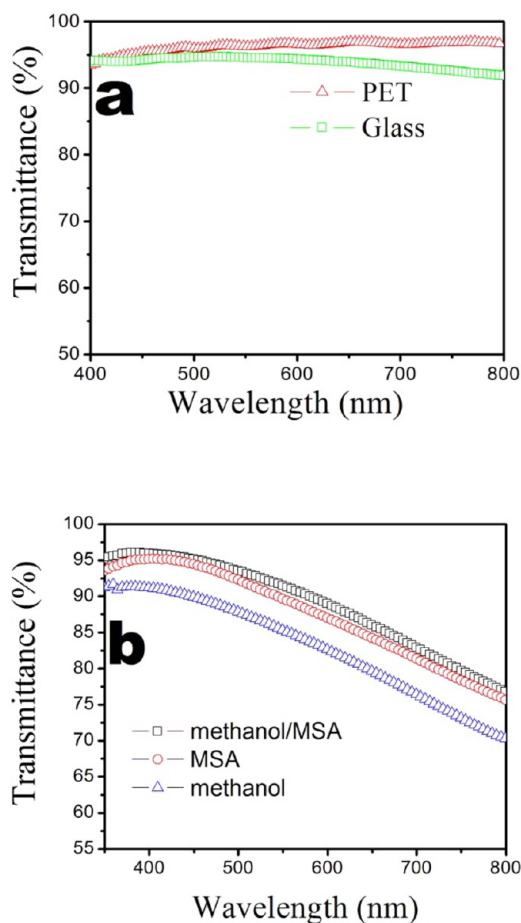


Figure 3. (a) Transparent spectra of the glass substrates and the PET substrates. (b) Transparent spectra of the PEDOT:PSS films on the PET substrates.

Except the film morphology as shown in Figure 2, PEDOT crystallinity also plays a critical role on the improvement of the film conductivity. Recently, Kim et al. reported that the conductivity performance of PEDOT:PSS films were also improved via enhancing the crystallinity of the PEDOT.³⁷ The crystallinity of PEDOT is determined by the peak intensity at 3.7 and 7.0°, which correspond to the lamella stacking distance $d(100)$ of two distinct alternate orderings of PEDOT and PSS.³⁷ Figure 4 shows the XRD spectra of all the PEDOT:PSS films treated by methanol and MSA. The as-cast films and the methanol-treated films have not any diffraction peaks, demonstrating much low crystallinity of PEDOT in the two films. However, the films with the MSA treatment have a strong diffraction peak at 7.1° and a weak peak shoulder at about 3.7°, whereas the methanol/MSA-treated films exhibit two strong diffraction peaks at 3.7 and 6.7°, demonstrating a large enhancement in crystallinity of PEDOT. Moreover, after the combined treatment, the peak at $2\theta = 7.1^\circ$ was shifted to a lower angle by about 0.4° with an increased intensity in the XRD spectra, which indicates an increased lamella stacking distance and an improved crystallinity. Ordered crystalline PEDOT conformation was induced from a coiled structure to a linear/extended-coil structure, which allows more interchain interaction between the PEDOT conducting polymers. Obviously, the results present that the combined treatment is superior to the single treatment for enhancing the film transparency and the crystallinity of PEDOT. The high

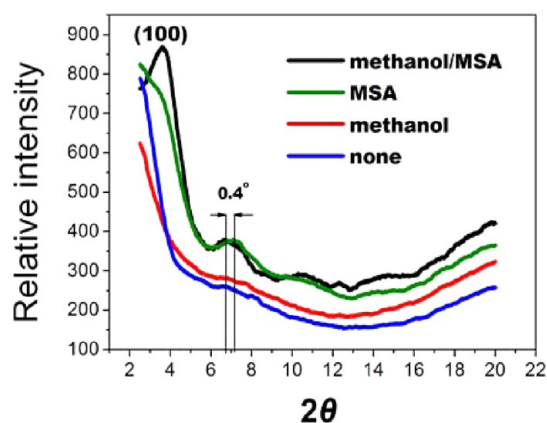


Figure 4. XRD spectra of the pristine PEDOT:PSS films and the PEDOT:PSS films treated by methanol, MSA, and methanol/MSA, respectively.

crystallinity of the PEDOT chains and the good phase separated morphology of the methanol/MSA-treated films can make the charge hopping easier, and eventually there is a tremendous enhancement in conductivity. To clarify these mechanisms of the conductivity enhancement, more experiments need be conducted in the future.

3.4. Effect of Methanol and MSA on the Photovoltaic Performance of OSCs. A high conductivity of PEDOT:PSS films along with a transparency of beyond 80% in the visible range satisfies its function as the transparent electrodes. Thus, the PEDOT:PSS film in the work can be applied to replace ITO as transparent electrodes in organic electronics. As is well-known, P3HT:PCBM is the most commonly used and classic photoactive layer in bulk heterojunction OSC devices. Here, we fabricated the bendable ITO-free OSCs with a structure of PET/conductive PEDOT:PSS films/PEDOT:PSS (Clevis P VP 4083)/P3HT:PCBM/Ca/Al, and the rigid OSCs with a rigid structure of Glass/ITO/PEDOT:PSS (Clevis P VP 4083)/P3HT:PCBM/Ca/Al. All the OSC devices were not encapsulated by ethoxyline resin for the next flexibility measurement. The effect of the methanol, MSA and methanol/MSA treatments on the photovoltaic performance of the devices is investigated.

Figure 5a shows the J - V curves of the bendable OSCs with the PEDOT:PSS films and the rigid OSCs with ITO-coated glass substrates under the illumination of AM1.5G, 100 mW cm^{-2} . Obviously, the photovoltaic performance of the bendable devices is improved significantly by using the combined treatment of methanol/MSA. The devices with the methanol treatment and the MSA treatment only exhibit a low relatively power conversion efficiency (PCE) of 3.51 and 3.58% with a short-circuit current density (J_{SC}) of 9.58 and 10.04 mA cm^{-2} , respectively. After the combined treatment of methanol/MSA, the J_{SC} increases to 10.18 mA cm^{-2} , and the PCE increases to 3.92%. The compensation in PCE of the methanol/MSA-treated OSC devices almost arises from the enhanced J_{SC} and fill factor (FF), which is attributed to the achievement of the higher conductivity of the PEDOT:PSS films, and the lower series resistance of the bendable devices. In the study, a dramatic improvement in conductivity from 1600 to 3560 S cm^{-1} , and a decrease in series resistance from 10.9 $\Omega \text{ cm}^2$ to 3.85 $\Omega \text{ cm}^2$ were observed in the films on the PET substrates, which contributed to the large enhancement of the OSC performance. To the best of our knowledge, the PCE of 3.92%

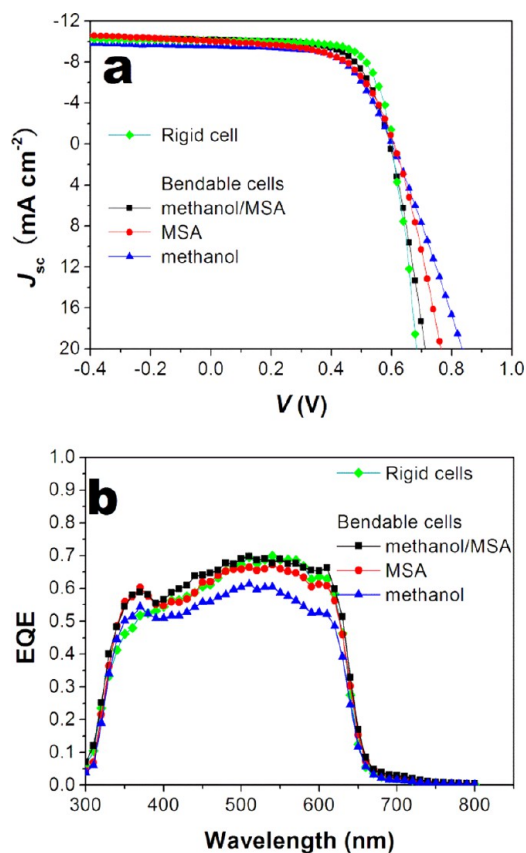


Figure 5. (a) J - V curves and (b) EQE spectra of the bendable OSCs with the PEDOT:PSS films and the rigid OSCs under the illumination of an AM 1.5G solar simulator, 100 mW cm^{-2} .

with open circuit voltage (V_{OC}) of 0.595 V, J_{SC} of 10.18 mA cm^{-2} , and FF of 0.65 for the bendable ITO-free OSC devices is among of the best values reported in literature for the P3HT:PCBM-based bendable solar cells. Based on the highly conductive films, more efficient OSCs with plastic substrates can be fabricated by using low-band gap polymers instead of P3HT for further applications.

For a reference, we also fabricated the rigid OSC devices with ITO-coated glass substrates. In comparison with the bendable ITO-free OSC devices with the optimized PEDOT:PSS films, the rigid devices exhibit an enhanced slightly PCE of 4.30% with V_{OC} of 0.600 V, J_{SC} of 10.09 mA cm^{-2} , FF of 71%. Our results demonstrate that the PEDOT:PSS films serve as promising electrodes for the fabrication of efficient and bendable ITO-free OSCs, which have a comparable performance to that of rigid electronics. Moreover, the technique of the methanol/MSA treatment is very important for roll to roll fabrication of large area and flexible electrodes in future applications.

Figure 5b shows the external quantum efficiency spectra of the bendable OSC devices with the structure of PET/Highly conductive PEDOT:PSS/PEDOT:PSS (Clevis P VP 4083)/P3HT:PCBM/Ca/Al and the rigid OSC devices with the structure of Glass/ITO/PEDOT:PSS (Clevis P VP 4083)/P3HT:PCBM/Ca/Al, under the illumination of an AM 1.5G solar simulator, 100 mW cm^{-2} . It is seen that the EQE values are consistent with the J_{SC} for the bendable devices and the rigid devices. The maximum EQE value reached 67.5% at 540 nm for the bendable devices, which demonstrates the highest J_{SC} of 10.18 mA cm^{-2} . The EQE value at 540 nm is reduced to

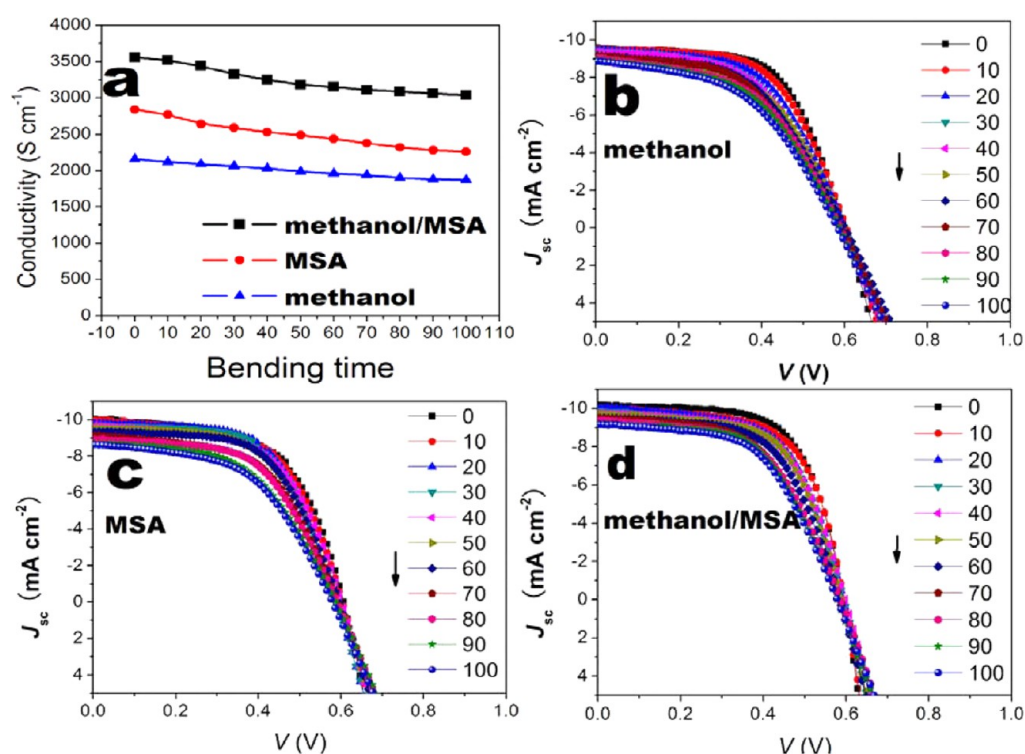


Figure 6. (a) Conductivity of the PEDOT:PSS films treated by methanol, MSA and methanol/MSA, respectively, as a function of bending times. Corresponding J - V curves of the bendable OSC devices with the films treated by (b) methanol, (c) MSA, and (d) methanol/MSA, respectively.

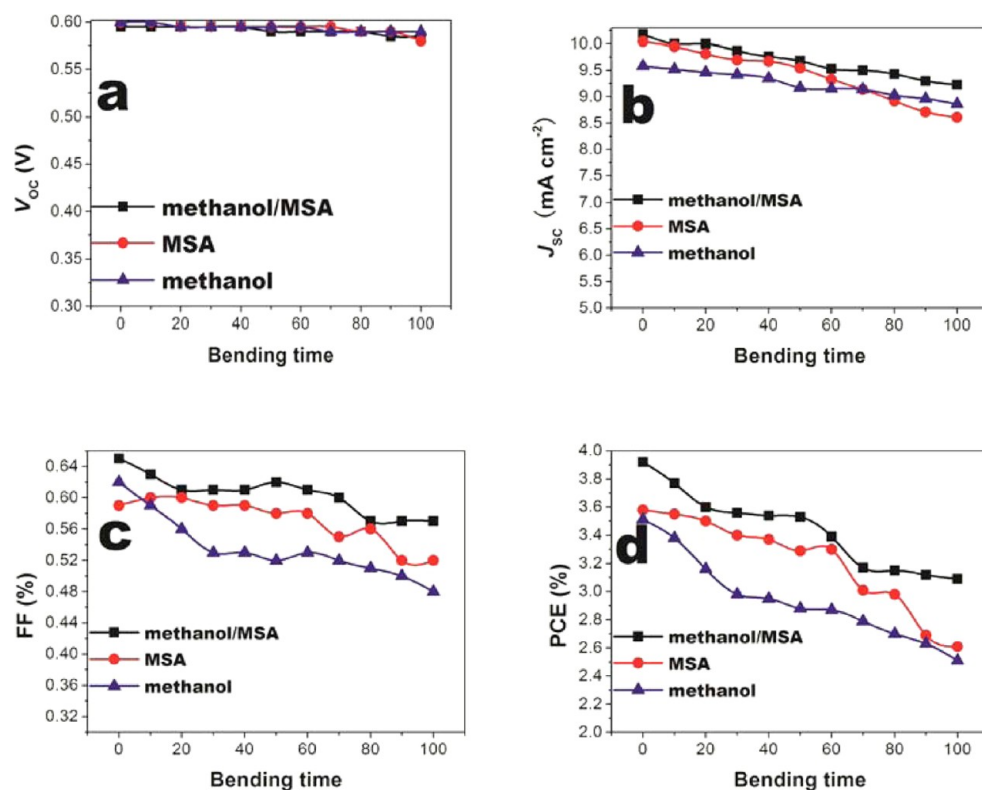


Figure 7. Variation of performance parameters of the bendable OSC devices as a function of the bending times; (a) V_{oc} , (b) J_{sc} , (c) FF, and (d) PCE.

62.5% for the bendable ITO-free devices with the methanol/MSA-treated PEDOT:PSS films, which show the J_{sc} of 9.58 mA cm^{-2} . Whereas the maximum EQE value of the rigid devices reach 70.0% at 540 nm, however, there is a sharp

decrease in EQE values below the wavelength of 500 nm, leading to the achievement of the J_{sc} of 10.09 mA cm^{-2} . Our results demonstrate that the optimized ITO-free devices are comparable to the ITO-based devices and are superior to the

bendable devices with the methanol-treated or the MSA-treated PEDOT:PSS films.

3.5. Effect of Mechanical Flexibility on Device Performance. The primary advantage of the OSCs with the electrode of PEDOT:PSS coated on the plastic substrates is that they continue to operate even when subjected to mechanical bending. In this work, the PEDOT:PSS films have a good repeatability in conductivity and can keep a long-term stability. However, a little decay of the conductivity still occurred when the films were bent in the ambient atmosphere.

Figure 6a show the conductivity of PEDOT:PSS films treated by methanol, MSA and methanol/MSA, respectively, as a function of the bending times. Variation trends of the film conductivity according to the bending times are demonstrated. The methanol-treated films and the methanol/MSA-treated films show a lower decay rate than the MSA-treated films. After the film was bent 100 times in the ambient atmosphere, the film conductivity dropped about 13.0 and about 14.6% of the initial conductivity for the methanol-treated films and for the methanol/MSA-treated films, respectively, whereas the MSA-treated films dropped about 20.4% of the initial results. The trends in conductivity of the films play a significant role of affecting the performance of the OSC devices when bent. Besides, the overall performance degradation of the bending devices without encapsulation mostly result from the break of the Ca/Al electrodes, as shown in Figure S2 (Supporting Information). It shows a breaking phenomenon of the Ca/Al film after bending, suggesting the easy oxidation of Ca films by the ambient atmosphere, which can lead to the degradation of device performance. Moreover, after the bending treatment, a buckled PEDOT:PSS film with a lower conductivity is proposed as a possible reason for the performance degradation. The factors contribute to the overall performance degradation.

The device performance as a function of the bending times is investigated here. Figure 6b–d present all the J – V curves of the bendable OSC devices with the different PEDOT:PSS films as a function of the bending times up to 100 times. The photovoltaic parameters derived from these J – V curves, the V_{OC} , the J_{SC} , the FF, and the PCE are plotted in Figure 7 for a clear comparison. Table 2 shows the performances of the bendable devices before and after the bending treatment, and the rigid devices with ITO on glass substrates. Obviously, the front devices with the methanol/MSA-treated PEDOT:PSS films show a lower decay rate of PCE than the latter devices with the PEDOT:PSS films only by the MSA treatment. After

Table 2. Photo-Voltaic Performances of the Bendable Devices with PEDOT:PSS Films and the Rigid Devices with ITO on Glass Substrates

devices	V_{OC} (V)	J_{SC} (mA cm ⁻²)	FF (%)	PCE (%)	change in PCE	R_s Ω cm ²
methanol	0.600	9.58	0.61	3.51	±0.06%	10.9
methanol and Bending	0.590	8.86	0.48	2.51	±0.08%	22.7
MSA	0.600	10.04	0.60	3.58	±0.05%	5.00
MSA and bending	0.580	8.61	0.52	2.61	±0.10%	16.7
methanol/MSA	0.595	10.18	0.65	3.92	±0.05%	3.85
methanol/MSA and bending	0.585	9.23	0.57	3.09	±0.11%	15.4
ITO on glass	0.600	10.09	0.71	4.30	±0.05%	2.83

the films were bent 100 times, the PCE of the front devices dropped about 21.2% of the initial value, whereas the PCE of the latter devices dropped 27.1% of the initial PCE. These trends in the device performance indicate that the combined treatment further improves the flexibility and the stability of the bendable ITO-free OSC devices. Moreover, it presents that a gradual decrease in PCE with the increase of the bending times, which is contributed by the loss in J_{SC} and in FF for all the bendable OSC devices. The PCE values decrease with the decrease in conductivity of the PEDOT:PSS films as well as the series resistance of the devices, suggesting that the decayed conductivity restrains charge carrier transport and collection by electrodes. However, the devices still maintain most of the performance through mechanical bending up to 100 times in the ambient atmosphere. Our devices are believed to tolerate repeated mechanical deformation in the long term when given a bending processing and J – V measurements in glove-boxes filled with protective gases (e.g., nitrogen and argon).

4. CONCLUSION

The PEDOT:PSS films on glass substrates and on PET plastic substrates were prepared with the combined treatments of methanol/MSA, and they exhibit an enhanced drastically conductivity up to 4800 and 3560 S cm⁻¹, respectively, which is mainly attributed to the achievement of highly ordered crystallinity of PEDOT and the removal of PSS from the PEDOT:PSS film matrix. Moreover, we fabricated the bendable ITO-free devices with P3HT as donor, PCBM as acceptor, the PEDOT:PSS films as positive electrode and Ca/Al as negative electrode. The optimized PEDOT:PSS films present a good mechanical flexibility that enables bendable ITO-free devices folding. The bendable devices not only show a relatively high PCE of 3.92% but also keep about 80% of the initial PCE after bending 100 times with large amplitude in the ambient atmosphere, due to the achievement of a relatively low series resistance and a good mechanical flexibility of the devices. Our results suggest that the highly conductive and flexible PEDOT:PSS films have substantial promise for high-performance and bendable ITO-free electronics.

■ ASSOCIATED CONTENT

Supporting Information

Resistance values of the treated films on glass substrates: EG, methanol, MSA, EG/MSA, and methanol/MSA; Ca/Al films without any bending treatment, Ca/Al films after the 100 time bending treatment. The Supporting Information is available free of charge on the ACS Publications website at DOI: 10.1021/acsami.5b02830.

■ AUTHOR INFORMATION

Corresponding Author

*E-mail: nanoguy@126.com.

Notes

The authors declare no competing financial interest.

■ ACKNOWLEDGMENTS

The authors would like to thank Dr. Hao Long for discussion. This work was financially supported by the National Nature Science Foundation of China (No. 51372075), the Nature Science Foundation of Hubei Province of China (No. 2015CFB354), and Research Fund for the Doctoral Program of Higher Education of China (RFDP, No. 20124208110006).

■ REFERENCES

- (1) Chipman, A. A Commodity No More. *Nature* **2007**, *449*, 131–131.
- (2) Hecht, D. S.; Hu, L.; Irvin, G. Emerging Transparent Electrodes Based on Thin Films of Carbon Nanotubes, Graphene, and Metallic Nanostructures. *Adv. Mater.* **2011**, *23*, 1482–1513.
- (3) Espinosa, N.; Garcia-Valverde, R.; Urbina, A.; Krebs, F. C. Life-cycle Analysis of Product Integrated Polymer Solar Cells. *Energy Environ. Sci.* **2011**, *4*, 1547–1557.
- (4) Xia, Y.; Sun, K.; Ouyang, J. Solution-Processed Metallic Conducting Polymer Films as Transparent Electrode of Optoelectronic Devices. *Adv. Mater.* **2012**, *24*, 2436–2440.
- (5) Zhang, W. F.; Zhao, B. F.; He, Z. C.; Zhao, X. M.; Wang, H. T.; Yang, S. F.; Wu, H. B.; Cao, Y. High-efficiency ITO-Free Polymer Solar Cells Using Highly Conductive PEDOT:PSS/surfactant Bilayer Transparent Anodes. *Energy Environ. Sci.* **2013**, *6*, 1956–1964.
- (6) Alemu, D.; Wei, H. Y.; Ho, K. C.; Chu, C. W. Highly Conductive PEDOT:PSS Electrode by Simple Film Treatment with Methanol for ITO-free Polymer Solar Cells. *Energy Environ. Sci.* **2012**, *5*, 9662–9671.
- (7) Kim, Y. H.; Sachse, C.; Machala, M. L.; May, C.; Müller-Meskamp, L.; Leo, K. Highly Conductive PEDOT:PSS Electrode with Optimized Solvent and Thermal Post-Treatment for ITO-Free Organic Solar Cells. *Adv. Funct. Mater.* **2011**, *21*, 1076–1081.
- (8) Lee, M. W.; Lee, M. Y.; Choi, J. C.; Park, J. S.; Song, C. K. Fine Patterning of Glycerol-doped PEDOT:PSS on Hydrophobic PVP Dielectric with Ink Jet for Source and Drain Electrode of OTFTs. *Org. Electron.* **2010**, *11*, 854–859.
- (9) Na, S. I.; Wang, G.; Kim, S. S.; Kim, T. W.; Oh, S. H.; Yu, B. K.; Lee, T.; Kim, D. Y. Evolution of Nanomorphology and Anisotropic Conductivity in Solvent-Modified PEDOT:PSS Films for Polymeric Anodes of Polymer Solar Cells. *J. Mater. Chem.* **2009**, *19*, 9045–9053.
- (10) Hsiao, Y. S.; Whang, W. T.; Chen, C. P.; Chen, Y. C. High-conductivity Poly(3,4-ethylenedioxythiophene):Poly(styrene sulfonate) Film for Use in ITO-free Polymer Solar Cells. *J. Mater. Chem.* **2008**, *18*, 5948–5955.
- (11) Kim, Y. S.; Oh, S. B.; Park, J. H.; Cho, M. S.; Lee, Y. Highly Conductive PEDOT/Silicate Hybrid Anode for ITO-free Polymer Solar Cells. *Sol. Energy Mater. Sol. Cells* **2010**, *94*, 471–477.
- (12) Na, S. I.; Kim, S. S.; Jo, J.; Kim, D. Y. Efficient and Flexible ITO-Free Organic Solar Cells Using Highly Conductive Polymer Anodes. *Adv. Mater.* **2008**, *20*, 4061–4067.
- (13) Ouyang, J.; Yang, Y. Conducting Polymer as Transparent Electric Glue. *Adv. Mater.* **2006**, *18*, 2141–2144.
- (14) Ouyang, J.; Chu, C. W.; Chen, F. C.; Xu, Q.; Yang, Y. High-Conductivity Poly(3,4-ethylenedioxythiophene):Poly(styrene sulfonate) Film and Its Application in Polymer Optoelectronic Devices. *Adv. Funct. Mater.* **2005**, *15*, 203–208.
- (15) Argun, A. A.; Cirpan, A.; Reynolds, J. R. The First Truly All-Polymer Electrochromic Devices. *Adv. Mater.* **2003**, *15*, 1338–1341.
- (16) Zhang, F.; Johansson, M.; Andersson, M. R.; Hummelen, J. C.; Inganäs, O. Polymer Photovoltaic Cells with Conducting Polymer Anodes. *Adv. Mater.* **2002**, *14*, 662–665.
- (17) Wu, Z.; Chen, Z.; Du, X.; Logan, J. M.; Sippel, J.; Nikolou, M.; Kamaras, K.; Reynolds, J. R.; Tanner, D. B.; Hebard, A. F.; Rinzler, A. G. Transparent, Conductive Carbon Nanotube Films. *Science* **2004**, *305*, 1273–1276.
- (18) Zhang, M.; Fang, S.; Zakhidov, A. A.; Lee, S. B.; Aliev, A. E.; Williams, C. D.; Atkinson, K. R.; Baughman, R. H. Strong, Transparent, Multifunctional, Carbon Nanotube Sheets. *Science* **2005**, *309*, 1215–1219.
- (19) Gruner, G. Carbon Nanotube Films for Transparent and Plastic Electronics. *J. Mater. Chem.* **2006**, *16*, 3533–3539.
- (20) Kim, K. S.; Kim, K. S.; Zhao, Y.; Jang, H.; Lee, S. Y.; Kim, J. M.; Kim, K. S.; Ahn, J. H.; Kim, P.; Choi, J. Y.; Hong, B. H. Large-Scale Pattern Growth of Graphene Films for Stretchable Transparent Electrodes. *Nature* **2009**, *457*, 706–710.
- (21) Becerril, H. A.; Mao, J.; Liu, Z.; Stoltenberg, R. M.; Bao, Z.; Chen, Y. Evaluation of Solution-processed Reduced Graphene Oxide Films as Transparent Conductors. *ACS Nano* **2008**, *2*, 463–470.
- (22) Gomez De Arco, L.; Zhang, Y.; Schlenker, C. W.; Ryu, K.; Thompson, M. E.; Zhou, C. Continuous, Highly Flexible, and Transparent Graphene Films by Chemical Vapor Deposition for Organic Photovoltaics. *ACS Nano* **2010**, *4*, 2865–2873.
- (23) Yu, Z.; Zhang, Q.; Li, L.; Chen, Q.; Niu, X.; Liu, J.; Pei, Q. Highly Flexible Silver Nanowire Electrodes for Shape-Memory Polymer Light-Emitting Diodes. *Adv. Mater.* **2011**, *23*, 664–668.
- (24) Lee, J. Y.; Connor, S. T.; Cui, Y.; Peumans, P. Solution-processed Metal Nanowire Mesh Transparent Electrodes. *Nano Lett.* **2008**, *8*, 689–692.
- (25) Zhu, R.; Chung, C.-H.; Cha, K. C.; Yang, W.; Zheng, Y. B.; Zhou, H.; Song, T.-B.; Chen, C.-C.; Weiss, P. S.; Li, G.; Yang, Y. Fused Silver Nanowires with Metal Oxide Nanoparticles and Organic Polymers for Highly Transparent Conductors. *ACS Nano* **2011**, *5*, 9877–9882.
- (26) Kim, J. Y.; Jung, J. H.; Lee, D. E.; Joo, J. Enhancement of Electrical Conductivity of Poly(3,4-Ethylenedioxythiophene)/Poly(4-styrenesulfonate) by A Change of Solvents. *Synth. Met.* **2002**, *126*, 311–316.
- (27) Huang, J.; Miller, P. F.; Wilson, J. S.; de Mello, A. J.; de Mello, J. C.; Bradley, D. D. C. Investigation of the Effects of Doping and Post-deposition Treatments on The Conductivity, Morphology, and Work Function of Poly(3,4-ethylenedioxythiophene)/Poly(styrene sulfonate) Films. *Adv. Funct. Mater.* **2005**, *15*, 290–296.
- (28) Zhou, Y.; Cheun, H.; Choi, S.; Potscavage, W. J.; Fuentes-Hernandez, C.; Kippelen, B. Indium Tin Oxide-free and Metal-free Semitransparent Organic Solar Cells. *Appl. Phys. Lett.* **2010**, *97*, 153304.
- (29) Badre, C.; Marquant, L.; Alsayed, A. M.; Hough, L. A. Highly Conductive Poly(3,4-ethylenedioxythiophene):Poly(styrenesulfonate) Films Using 1-Ethyl-3-methylimidazolium Tetracyanoborate Ionic Liquid. *Adv. Funct. Mater.* **2012**, *22*, 2723–2727.
- (30) Vosgueritchian, M.; Lipomi, D. J.; Bao, Z. Highly Conductive and Transparent PEDOT:PSS Films with A Fluorosurfactant for Stretchable and Flexible Transparent Electrodes. *Adv. Funct. Mater.* **2012**, *22*, 421–428.
- (31) Ko, C.-J.; Lin, Y.-K.; Chen, F.-C.; Chu, C.-W. Modified Buffer Layers for Polymer Photovoltaic Devices. *Appl. Phys. Lett.* **2007**, *90*, 063509.
- (32) Peng, B.; Guo, X.; Cui, C.; Zou, Y.; Pan, C.; Li, Y. Performance Improvement of Polymer Solar Cells by Using A Solvent-treated Poly(3,4-ethylenedioxythiophene):Poly(styrenesulfonate) Buffer Layer. *Appl. Phys. Lett.* **2011**, *98*, 243308.
- (33) Xia, Y.; Zhang, H. M.; Ouyang, J. Highly Conductive PEDOT:PSS Films Prepared through A Treatment with Zwitterions and Their Application in Polymer Photovoltaic Cells. *J. Mater. Chem.* **2010**, *20*, 9740–9747.
- (34) Kim, N.; Kee, S.; Lee, S. H.; Lee, B. H.; Kahng, Y. H.; Jo, Y.-R.; Kim, B.-J.; Lee, K. Highly Conductive PEDOT:PSS Nanofibrils Induced by Solution-Processed Crystallization. *Adv. Mater.* **2014**, *26*, 2268–2272.
- (35) Ouyang, J. Solution-Processed PEDOT:PSS Films with Conductivities as Indium Tin Oxide through A Treatment with Mild and Weak Organic Acids. *ACS Appl. Mater. Interfaces* **2013**, *5*, 13082–13088.
- (36) Gong, C.; Yang, H. B.; Song, Q. L.; Lu, Z. S.; Li, C. M. Mechanism for Dimethylformamide-treatment of Poly(3,4-ethylenedioxythiophene):Poly(styrene sulfonate) Layer to Enhance Short Circuit Current of Polymer Solar Cells. *Sol. Energy Mater. Sol. Cells* **2012**, *100*, 115–119.
- (37) Kim, N.; Lee, B. H.; Choi, D.; Kim, G.; Kim, H.; Kim, J.-R.; Lee, J.; Kahng, Y. H.; Lee, K. Role of Interchain Coupling in the Metallic State of Conducting Polymers. *Phys. Rev. Lett.* **2012**, *109*, 106405.